Desalination and Water Treatment
www.deswater.com
doi: 10.1080/19443994.2013.812521

52 (2014) 5912–5922
September

Taylor & Francis
Taylor & Francis Group

Biosorption of Cr^{6+} from aqueous solution by sugarcane bagasse

Inés de la C. Alomá[a], I. Rodríguez[a], M. Calero[b,*], G. Blázquez[b]

[a]*Department of Chemical Engineering, Central University "Marta Abreu" of Las Villas, Carretera a Camajuaní km 5 [1/2], Santa Clara, Villa Clara, Cuba*
[b]*Department of Chemical Engineering, University of Granada, 18071 Granada, Spain*
Tel. +34 958 243311; Fax: +34 958 248992; email: mcaleroh@ugr.es

Received 1 January 2013; Accepted 29 May 2013

ABSTRACT

The biosorption characteristics of Cr^{6+} from aqueous solution using sugarcane bagasse (SCB) were investigated. Experimental parameters affecting the biosorption process, such as pH, contact time, initial metal concentration, and temperature were studied. The equilibrium nature of Cr^{6+} biosorption at different temperatures was described by the Freundlich, Langmuir, Sips, and Dubinin–Radushkevich isotherms. The biosorption isotherm of SCB for Cr^{6+} followed the Langmuir model, and the maximum biosorption capacity of Cr^{6+} obtained was 1.76 mg/g at 25°C. The biosorption kinetics of Cr^{6+} onto SCB followed the pseudo-second-order model. The calculated thermodynamic parameters (ΔG, ΔH, and ΔS) showed that the biosorption of Cr^{6+} ions were feasible, spontaneous ($\Delta G = -21.52\,\text{kJ}\cdot\text{mol}^{-1}$), and exothermic ($\Delta H = -6.364\,\text{kJ}\cdot\text{mol}^{-1}$) at the temperature range of 25–65°C.

Keywords: Sugarcane bagasse; Biosorption; Heavy metals; Equilibrium isotherm; Kinetic

1. Introduction

Toxic metals are often discharged by a number of industrial processes, such as electroplating, leather tanning, textile dyeing, and metal finishing industries, and this can lead in turn to the contamination of freshwater and marine environment. According to water standards used in most countries, levels of heavy metal ions in wastewater must be controlled and reduced to a set value.

Heavy metal contamination has gained much attention due to its potential health impact on the public [1]. Among these heavy metals, chromium is considered highly poisonous, toxic, and carcinogenic by the US EPA (environmental protection agency) [2]. The recommended limit of Cr^{6+} in potable water is 0.1 mg/L [3]. Therefore, removal of Cr^{+6} from water and wastewater has been a great challenge for environmental scientists [4]. Compounds of Cr^{6+} are very mobile, so they readily enter into underground waters and make them poisonous.

There are several methods available to achieve the removal of heavy metals in wastewater [5]. The most common method is chemical precipitation; this method requires relatively high amount of chemical usage, accumulation of concentrated sludge with obvious disposal problems, and expensive plant requirements or operational costs. Other processes include chemical coagulation/flocculation, oxidation, ion exchange, and precipitation. These methods are relatively expensive, with high costs of operation and energy requirements [6].

---

*Corresponding author.

Several researches in biosorption suggests the following advantages over other techniques: the materials can be found easily as wastes or byproducts and at almost no cost; there is no need of costly growth media; the process is independent of physiological constraints of living cells; process is very rapid, as non-living material behaves as an ion-exchange resin, and metal loading is very high; the conditions of the process are not limited by the living biomass, no aseptic conditions are required; process is reversible and metal can be desorbed easily, thus recycling of the materials is quite possible; chemical or biological sludge is minimized. However, there are certain disadvantages as well: irrespective of the value of the metal, it needs to be desorbed from the material to be further re-employed; the characteristics of the biosorbents cannot be biologically controlled [7].

The majority of recent biosorption studies were conducted with low-cost agricultural wastes such as, olive stone [8,9], lignin extracted from *Tithonia diversifolia* [10], rice straw [11], wheat shell [12], rice bran [13], *Moringa oleifera* leaves powder [14], or wood apple shell [15] and all of them have been identified as potential biosorbents for heavy metal removal. Sugarcane bagasse (SCB) is particularly interesting in its use, in several Latin American and Asian countries because of its high availability. SCB has around 50% cellulose, 27% polyoses, and 23% lignin and the interest in the use of bagasse as an adsorbent has been promoted by the good results that have been obtained [16,17].

The objectives of this research include: (1) to investigate the biosorption capacity of SCB for the removal of Cr^{6+} from aqueous solutions; (2) to optimize the different experimental conditions, such as temperature, pH of the solution, initial ion concentration, and contact time in order to understand the kinetic mechanism; and (3) to model the biosorption process.

This study optimized the experimental use of the SCB in their natural form, i.e. without any treatment, so that the results reflect their behavior as adsorbent of this solid, with the intrinsic contribution that they have their majority components, such as the lignin.

2. Materials and methods

2.1. Preparation of biosorbent

SCB is a waste byproduct from sugar milling. The sugarcane bagasse used in this work was supplied by the pilot plant "Jose´ Marti" located in Central University "Marta Abreu" of Las Villas, Cuba.

It was washed with distilled water several times and dried at 25˚C. No other chemical or physical treatments were used prior to biosorption experiments. Then, it was grinded with a strong grinder and sieved to 0.5–1 mm particle size.

2.2. Preparation of Cr^{6+} solutions

Analytical reagent grade of $K_2Cr_2O_7$ supplied by J.T. Baker was used by preparing the synthetic wastewater. It was prepared by diluting the $K_2Cr_2O_7$ with distilled water to desired concentrations. Then, the pH of the solution was adjusted to 2 by addition of NaOH (0.1 mol/L) or HCl (0.1 mol/L) solutions.

2.3. Analytical measurements

The percentages of carbon, hydrogen, nitrogen, and sulfur were determined using an EA 1108 CHNS elemental analyzer (Fison's Instruments). The oxygen content was obtained indirectly by difference.

An IR analysis was performed with a Fourier transform infrared spectrometer (Nicolet 20SBX) to identify the chemical groups present in the biosorbent and to complete the study of the functional groups. The experiment was carried out using KBr disks to prepare the SCB sample and the spectral range varied from 4,000 to 400 cm^{-1}.

The surface morphology of the solids was analyzed using a JEOL JSM—5,900 LV scanning electron microscope at an accelerating voltage of 5 kV and a working distance of 4 mm.

The thermal behavior of SCB was obtained by using a TGA-2950 thermogravimetric analyzer. About 10 mg of SCB was heated between 60 and 950˚C at 20˚C/min. First, the atmosphere used was N_2 with a flow rate of 20 mL/min. When the desired temperature (950˚C) was reached, the atmosphere was changed from inert (N_2) to oxidative (O_2) and temperature was held for 30 min at 950˚C for the burnout of any remaining carbon in the residue.

2.4. Batch biosorption experiments

2.4.1. Effect of pH solution, initial metal ion concentration, contact time, and temperature

The effect of pH on biosorption capacity of the SCB was investigated using 10 mg/L of Cr^{6+} concentration at pH range of 1–4 at 25˚C; 1.0 g of SCB was added to 100 mL of Cr^{6+} solutions. Flasks were agitated on a shaker for 40 min. Then, the mixture was centrifuged, filtrated, and the Cr^{6+} in the remaining solution was analyzed in an atomic absorption

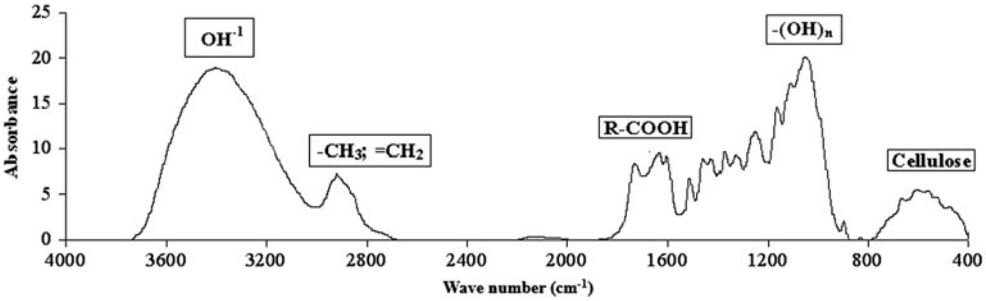

Fig. 1. Fourier transforms infrared (FTIR) spectra of SCB.

spectrometer (SpectrAA 220 SS. Model Varian).The Cr^{6+} removal percentage was calculated using the following equation:

$$\text{Removal}\,(\%) = \frac{C_o - C_e}{C_o} 100 \tag{1}$$

where C_o (mg/L) is the initial concentration and C_e (mg/L) is the equilibrium concentration.

The effect of the variation of Cr^{6+} initial concentration and contact time was studied using 100 mL of Cr^{6+} solution at concentrations from 10 to 140 mg/L, contact time from 3 to 120 min, pH 2.0, and biosorbent dosage of 10 g/L.

The biosorption equilibrium experiments were carried out using 100 mL of Cr^{6+} solution at concentrations from 10 to 140 mg/L, contact time 90 min, pH 2.0, biosorbent dosage 10 g/L, and temperatures of 25, 50, and 65˚C.

3. Result and discussion

3.1. Characterization of the biosorbent

3.1.1. Elemental analysis

Measurements of elemental analysis can be employed for understanding chemical properties of biosorbent. Elemental analysis results showed that SCB is composed of 43.03% carbon, 6.42% hydrogen, 0.60% nitrogen, <0.1% sulfur, and 49.95% oxygen. These results were obtained in a previous study [18]. The low percentage of nitrogen and sulfur suggest a limited presence of amine and sulfur groups in the biosorbent.

3.1.2. FTIR analysis

The FTIR technique is an important tool to identify some characteristic functional groups, which are capable of adsorbing metal ions.

The FTIR spectra of the solid samples are shown in Fig. 1. The characteristic IR bands for lignocellulosic materials, as sugarcane bagasse, can be divided into four regions: the broad hydroxyl bands (3,200–3,600 cm^{-1}), the stretching bands of CH, CH_2, and CH_3 (2,800–3,000 cm^{-1}), the stretching bands of carbonyl groups (1,550– 1,750 cm^{-1}), and the fingerprint region (below 1,550 cm^{-1}) in which the assignment of IR peaks is not clear because of the complex interaction of their vibration systems [19–22].

3.1.3. Scanning electron micrograph (SEM)

Results of scanning electron microscope of the surface morphology of SCB are given in Fig. 2. The morphology of SCB can facilitate the biosorption of metals, due to the irregular surface and different levels of porosity in the material, which makes possible the biosorption of Cr^{6+} in different parts of this material. Therefore, based on the morphology, as well as on the fact that high amounts (10.3%) of silica are located on the SCB [23,24], it can be concluded that this material is adequate to retain metal ions [19].

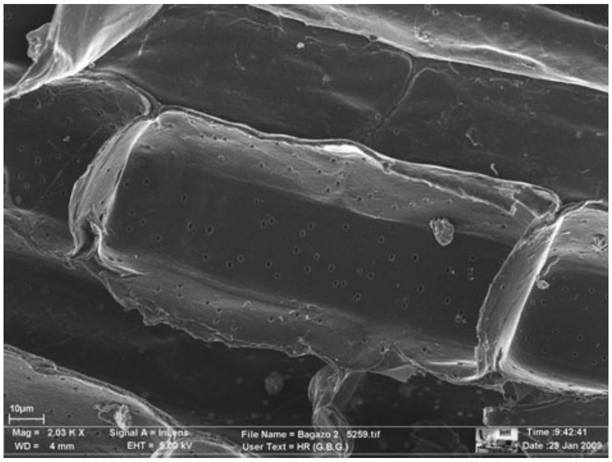

Fig. 2. Scanning electron micrographs of SCB. (Mag: 2.03 KX. EHT: 5.00 kV. WD = 4 mm).


Sample Temp 166.65 °C
Weight % 13.2523 %
Delta T -2.818 °C
Weight 2.530 mg
Weight % 13.2523 %
Approx. Gas Flo 19.6 ml/min
Time Remainin

Fig. 3. Thermogravimetric curve (TG) of SCB. For details, see text.

3.1.4. Thermogravimetric analysis

The thermal stability of SCB was examined by TGA. Thermal decomposition of SCB was performed under no isothermal conditions and under a constant heating rate of 20˚C/min.

The overall mass loss during thermogravimetric analysis can be divided into steps related to moisture, hemi-cellulose, cellulose, and lignin (Fig. 3). The first step is associated with a small weight loss (9%) due to dehydration which accounts for the moisture content by heating the sugarcane bagasse up to 250˚C. Afterwards, the second step of pyrolysis was obtained when the temperature was varied from 250 to 360˚C. In this step, a higher mass loss (60%) was observed. The behavior of the pyrolysis curve at this temperature indicates hemicellulose and cellulose decomposition, as well as loss of the remaining adsorbed water [25]. Lignin decomposition occurs in the 360–525˚C range, thus indicating that this structure presents higher stability than hemi-cellulose and cellulose. The final step begins with the introduction of O_2, at 950˚C, when an instant major weight loss is observed due to the burning of the residual carbon present in the residue; no mass loss was detected when the temperature was increased to 950˚C and this result indicates the presence of oxides (mainly those of aluminum and silicon), which are stable at higher temperatures.

From the TGA analyses of the biosorbent, it may be concluded that the biosorbent could be used even at higher temperatures in water treatment.

3.2. Batch biosorption studies

3.2.1. Effect of pH

The pH plays an important role in the biosorption process by affecting the surface charge of biosorbent, the degree of ionization, and speciation of the adsorbate [26]. Therefore, preliminary experiments have been performed to find out the optimum pH for maximizing the Cr^{6+} removal.

For discerning about the speciation of chromium, a chemical equilibrium program was used to calculate the speciation of chromium in the aqueous solution, based on thermodynamic data as a function of solution pH and for a total salt concentration of 10 mg/L (Fig. 4(a)) [27]. The results showed $HCrO^{-4}$ is the main specie present for pH values lower than 4, approximately. However, when the pH exceeds 4, concentration in solution decreases due the precipitation process [19,27].

The effect of pH of the solution on removal of Cr^{6+} using SCB is shown in Fig. 4(b) (metal concentration

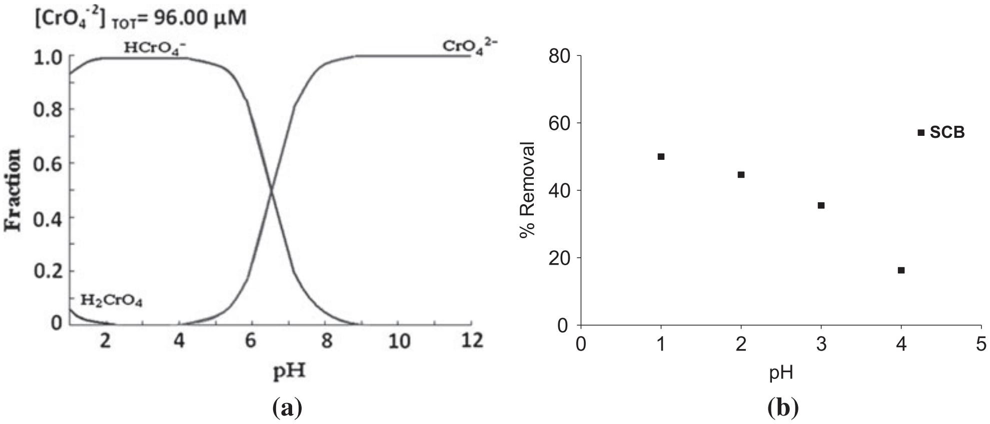

(a) (b)

Fig. 4. Effect of pH on the speciation of Cr^{6+} in solution (metal ion solubility) (a) Medusa software and (b) Experimental test (pH: 1–4, SCB dosage: 10 g/L, initial conc.: 10 mg/L, temperature: 25˚C, time: 40 min).

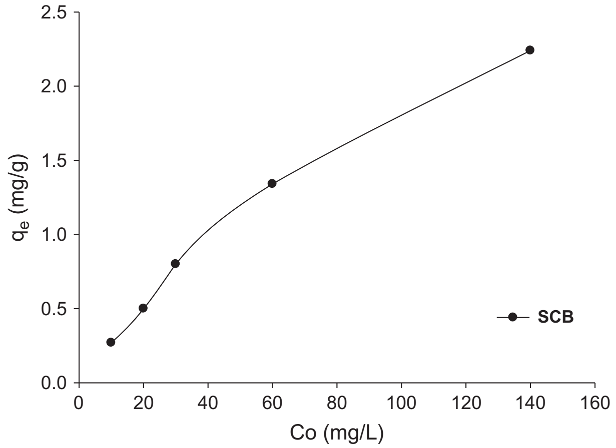

Fig. 5. Effect of initial concentration of Cr^{6+} on biosorption using SCB (pH: 2, SCB dosage: 10 g/L, initial conc.: 10–140 mg/L, temperature: 25℃, time: 90 min).

10 mg/L, SCB concentration 10 g/L, temperature 25℃, and contact time 40 min). From this figure, it becomes clear that the maximum percent of Cr^{6+} removal is obtained at pH 1.0 and decreases with further increase in pH. However, to avoid working with extreme pH values, a pH value of 2 has been selected for the remaining experiments.

This result is directly related with competition ability of hydrogen ions with metal ions to bind to the active sites on the adsorbent surface. Several mechanisms, such as electrostatic forces, ion exchange, and chemical complexation must be taken into account when examining the effect of pH on Cr^{6+} biosorption. One of the commonly proposed mechanisms is electrostatic attraction between sorbent and sorbate. At very low pH values, there is high concentration of H^+ ions, which in turn neutralizes the negatively charged adsorbent surface, thereby reducing hindrance to the diffusion of $HCrO^-{}_4$. When the pH increases, the concentration of OH^- ions increases and overall charge on surface of the sorbent becomes negative, which causes repulsion effect against the negatively charged Cr^{6+} species, such as $Cr_2O_7{}^{2-}$ and $CrO_4{}^{2-}$, and therefore results in the decreased biosorption of hexavalent chromium ions.

According to González et al. [28], the distribution of Cr(VI) and Cr(III) is strongly dependent on the pH of the solution, the initial metal concentration and the dosage of the biosorbent. All the species of chromium in the solution were in their trivalent form at $pH < 2$.

3.2.2. Effect of initial metal ion concentration

A given mass of adsorbent can adsorb only a fixed amount of adsorbate. So, the initial concentration of adsorbate solution is important. Fig. 5 shows the biosorption capacity of SCB (10 g/L) at various initial concentrations (10–140 mg/L) of Cr^{6+}. It can be seen that the amount of Cr^{6+} adsorbed per unit mass of adsorbent (SCB) increases with the increase in the initial concentration in test solution. This effect is explained by the decrease in resistance for the uptake of solute from solution with the increase in metal concentration.

Contact time between the metal and the adsorbent is relevant in wastewater treatment by biosorption. A rapid uptake of metal and the establishment of equilibrium in a short period imply an adsorbent efficient for its use in wastewater treatment.

3.2.3. Effect of temperature and contact time

To investigate the effect of the temperature (25, 50, and 65℃) and contact time on the Cr^{6+} biosorption, experiments were conducted using constant concentrations of Cr^{6+} (10 mg/L) at different times (0–120 min).

The results are given in Fig. 6. As can be seen from these figures, the biosorption of Cr^{6+} onto the surface of SCB occurred quickly, during the first 30 min, for three temperatures. Then, it was observed that the biosorption rate was constant after 90 min at all temperatures. The adsorbed amount of Cr^{6+} ions decreases with increasing temperatures from 25 to 65℃. The observed decrease in the biosorption capacity with an increase of temperature from 25 to 65℃ indicated that low temperatures favor Cr^{6+} ions removal by biosorption onto the SCB. These results show that the biosorption process is exothermic in nature.

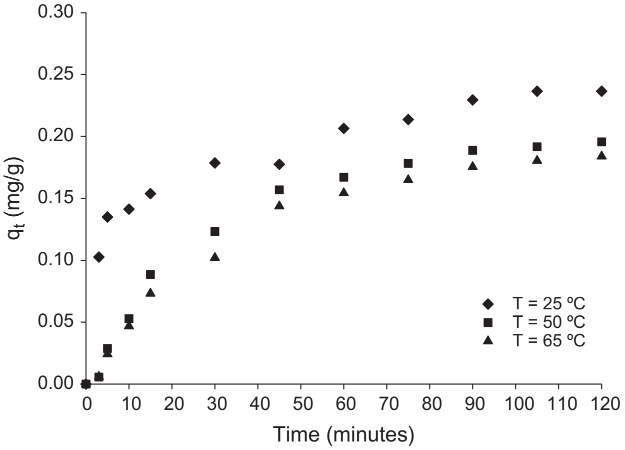

Fig. 6. The effect of contact time and temperature on the biosorption of Cr^{6+} (pH: 2, SCB dosage: 10 g/L, initial conc.: 10 mg/L, time: 0–120 min).

Similar results have also been reported for the biosorption of Pb (II) and Cr (III) of lichen biomass [29], removal of Cr (VI) onto heat-activated bauxite [30], and removal of Cr (VI) using micellar compound [31].

3.3. Batch kinetics models

In order to investigate the mechanism of biosorption, three different models have been used at different experimental conditions.

The most common models used to fit the kinetic biosorption experiments are Lagergren's pseudo-first-order model (Eq. 2) [32] and pseudo-second-order model (Eq. 3) [33]:

$$q_t = q_e\left(1 - e^{-k_1 t}\right) \tag{2}$$

$$q_t = \frac{t}{\frac{1}{K_{s2} q_e^2} + \frac{t}{q_e}} \tag{3}$$

where q_e (mg/g) and q_t (mg/g) are the amount of adsorbate adsorbed at equilibrium and at time t, respectively. k_1 (min^{-1}) and k_{s2} (g/mg.min) are the pseudo-first-order and pseudo-second-order biosorption rate constants, respectively. The initial biosorption rate, h ($\mathrm{mg{\cdot}g^{-1}{\cdot}min^{-1}}$) is $k_{s2}q_e{}^2$.

The intraparticle diffusion model proposed by Weber and Morris [34] is tested for the diffusion mechanism. The intraparticle equation can be described as [35,36]:

$$q_t = k_w \times t^{1/2} \tag{4}$$

where q_t is the amount of metal ions adsorbed at time t (mg/g) and k_W is the intraparticle diffusion rate constant ($\mathrm{mg/g{\cdot}min^{0.5}}$). If this model reproduces appropriately experimental data, the representation of q_t vs. $t^{1/2}$ should provide a straight line of slope k_w. Fig. 7 presents this plot. Model parameters were determined by nonlinear regression using the optimization method of the Solver function in a spreadsheet Excel.

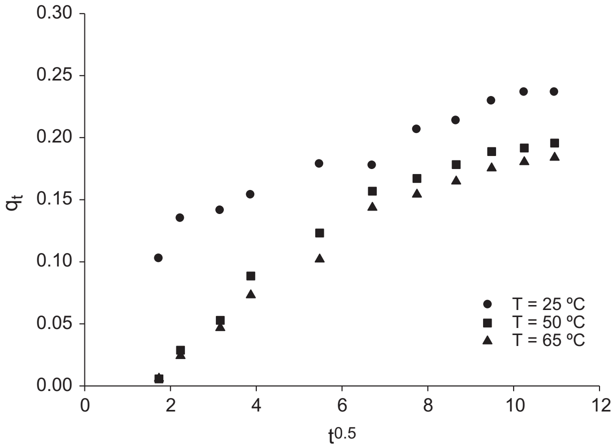

Fig. 7. Weber–Morris plots (pH: 2, SCB dosage: 10 g/L, time: 3–120 min, stirred-speed: 150 rpm).

Also, experiments have been performed for other initial concentrations of chromium by maintaining the temperature constant at 25˚C. The results are shown in Tables 1 and 2. It is observed that the temperature effect is not significant and the three models tested fit the experimental data rather well. The equilibrium biosorption capacity, q_e, decreased slightly with the increase in the temperature and the process became slower.

The pseudo-second-order kinetic models provided a good correlation for the biosorption of Cr^{6+} onto SCB for all the initial concentrations of Cr^{6+} tested, in contrast to the pseudo-first-order and Weber–Morris models. Although the intraparticle diffusion model is linear for an initial concentration of chromium of 10 mg/L (a linear plot of q_t vs. $t^{1/2}$ was observed, as designated in Fig. 7), the low r^2 for other concentrations indicate that the intraparticle diffusion model does not fit the data well. This tendency indicates that the rate limiting step is the chemisorption involving valence forces through the sharing or the exchange of electrons between sorbent and sorbate, complexation, coordination, and/or chelation [19,37].

Table 1
Kinetics parameters for removal of Cr^{6+} by biosorption onto SCB. ($C_o = 10$ mg/L, pH: 2, SCB dosage: 10 g/L, time: 3–120 min, stirred-speed: 150 rpm)

T (˚C)	Pseudo-first-order		Pseudo-second-order				Weber-Morris	
	k_1 (min^{-1})	R^2	k_{s2} (g/mg min)	q_e (mg/g)	h (mg/mg min)	R^2	k_W (mg/g $\mathrm{min}^{0.5}$)	R^2
25	0.029	0.92	0.47	0.27	0.034	0.90	0.014	0.97
50	0.033	0.99	0.12	0.26	0.008	0.99	0.021	0.92
65	0.028	0.99	0.094	0.25	0.006	0.99	0.020	0.96

Table 2
Kinetics parameters for removal of Cr^{6+} by biosorption onto SCB. (T: 25°C, pH: 2, SCB dosage: 10 g/L, time: 3–120 min, stirred-speed: 150 rpm)

C_0 (mg/L)	Pseudo-first-order		Pseudo-second-order				Weber-Morris	
	k_1 (min^{-1})	R^2	k_{s2} (g/mg min)	q_e (mg/g)	h (mg/mg min)	R^2	K_W (mg/g min$^{0.5}$)	R^2
10	0.029	0.92	0.47	0.27	0.034	0.90	0.014	0.97
20	0.050	0.94	0.66	0.50	0.17	0.99	0.023	0.82
30	0.086	0.97	0.09	0.80	0.060	0.98	0.025	0.88
60	0.056	0.93	0.10	1.34	0.18	0.99	0.044	0.77

The Fig. 8 presents the adjustment of the experimental data to the three kinetic models used for the biosorption of Cr^{6+} onto SCB at 25°C. It is appreciated that the pseudo-second-order model is the one that better reproduces the experimental data.

3.4. Biosorption isotherm

Several isotherm equations have been used for the equilibrium modeling of biosorption systems. Among these, two are commonly used and have been applied for this study, the Freundlich and Langmuir isotherms. Also, Dubinin–Radushkevich and Sips isotherm have been used.

The Langmuir isotherm model, given in Eq. (5), is representative of monolayer biosorption occurring on an energetically uniform surface on which the adsorbed molecules are not interactive [38–40]. Accordingly, equilibrium is attained once the monolayer is completely saturated [41]. The nonlinear model is transformed into Eq. (6) and the corresponding constants can be obtained.

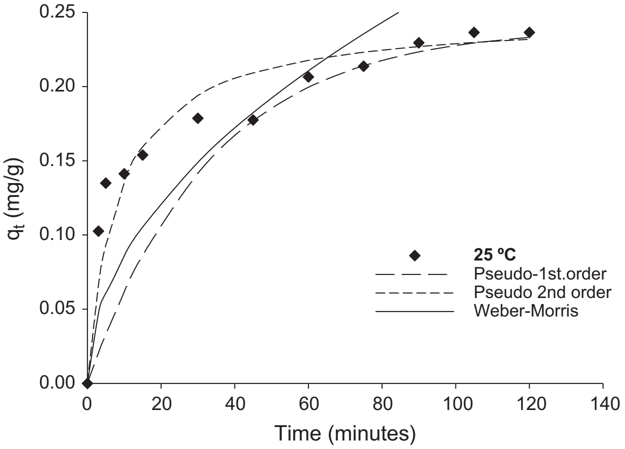

Fig. 8. The experimental and calculated kinetic (temperature: 25°C, pH: 2, SCB dosage: 10 g/L, time: 3–120 min, stirred-speed: 150 rpm).

$$q_e = \frac{q_{\max} \times k_{ads} \times C_e}{1 + k_{ads}C_e} \tag{5}$$

$$\frac{C_e}{q_e} = \frac{C_e}{q_{\max}} + \frac{1}{q_{\max} \times K_{ads}} \tag{6}$$

where q_e is the equilibrium biosorption capacity (mg/g), C_e is the equilibrium concentration of solution (mg/L), $q_{\max}$ is the Langmuir constant representing the maximum biosorption capacity (mg/g), and k_{ads} is the Langmuir constant related to the energy of biosorption (L/mg). The values of Langmuir constants $q_{\max}$ and k_{ads} were obtained from the intercept and slope of the plot between (C_e/q_e) vs. (C_e).

Contradictory to Langmuir, Freundlich model, shown in Eq. (7), describes the biosorption on an energetically heterogeneous surface on which the adsorbed molecules are interactive [26,42]. The model is linearized to give Eq. (8):

$$q_e = k_F \times C^{1/n} \tag{7}$$

$$\log q_e = \log k_F + \frac{1}{n} \log C_e \tag{8}$$

where k_F and n are constants for Freundlich isotherm that are indicative of the biosorption capacity (mg/ g) and intensity of the adsorbent, respectively [2,29]. The values of K_F and n were calculated from the slope and intercept of the plot between ln q_e and ln C_e.

The experimental data was fitted to Dubinin–Radushkevich (D–R) isotherm model in order to determine the biosorption type. Originally the D–R equation was developed as a semi-empirical tool to describe the adsorption isotherms of microporous materials based on the Polanyi potential theory of adsorption [43]. The nonlinear model given with Eq. (9) is reduced to the linear form as in Eq. (10).

$$q_e = q_{\max} \exp(-k_{D-R} \times \varepsilon^2) \tag{9}$$

$$\ln q_e = \ln q_{\max} - k_{D-R} \times \varepsilon^2 \quad (10)$$

where $q_{\max}$ is the maximum biosorption capacity (mg/g), k_{D-R} is a constant related to the energy of biosorption (mol^2/J^2), and ε is the Polanyi potential which is calculated from Eq. (11) [19,44].

$$\varepsilon = RT \ln\left(1 + \frac{1}{C_e}\right) \quad (11)$$

where R is the universal gas constant (J/mol·K) and T is temperature (K). The isotherm constants $q_{\max}$ and k_{D-R} were calculated from the slope and intercept of the plot of ln q_e vs. ε^2.

Sips [20] proposed an empirical isotherm equation, also known as Langmuir–Freundlich isotherm, which is often expressed as:

$$q_e = \frac{q_{\max} k_{ads} C_e^{1/n}}{1 + k_{ads} C_e^{1/n}} \quad (12)$$

where k_{ads} is the Sips constant (L/mg) and n is the heterogeneity coefficient. The Langmuir–Freundlich denomination derives from the limiting behavior of the equation. At low adsorbate concentrations, the Sips isotherm is effectively reduced to a Freundlich isotherm and thus does not obey Henry's law. At high adsorbate concentrations, it predicts a monolayer biosorption capacity characteristic of the Langmuir isotherm [21].

The computed constants are shown in Table 3. The experimental data exhibited high correlation with Langmuir model within the studied temperature range ($R^2 = 0.99$). Both $q_{\max}$ and k_{ads} decreased with the increase in temperature. Several researchers have reported decreasing Langmuir constants with temperature, for biosorption of Cr^{6+} on chitosan [38], red algae (*Ceramium virgatum*) [45], and *Turkish Vermiculite* [46].

All constants exhibited a decrease with the increase in temperature, which is an indication of the exothermic nature of the process. Examination of the regression coefficients proved that the correlation of Langmuir model was stronger with respect to Freundlich model for the temperatures studied.

From the Dubinin–Radushkevich isotherm, the data were not consistent with the model ($R^2 < 0.90$). The value of k_{D-R} calculated was $4.48 \cdot 10^{-3}$ mol^2/kJ^2 at 25°C. The mean free energy of biosorption (E) was calculated using the value of k_{D-R} according to Eq. (13).

$$E = \frac{1}{\sqrt{2 \times k_D - R}} \quad (13)$$

The values of E give information about the biosorption mechanism as chemical ion exchange or physical biosorption. If its values are in the range of 8–16 kJ/mol, the biosorption process follows chemical ion exchange mechanism while for the values < 9 kJ/mol, the biosorption process is of a physical nature. The values of E were found to be 10.6, 11.8, and 12.0 kJ/mol for 25, 50, and 65°C, respectively. Consequently, it is reasonable to suggest that the Cr^{6+} biosorption onto SCB probably may occur by chemical ion-exchange process [19].

The values of k_{ads} parameter from Sips isotherm increased with the increase in temperatures (Table 3). This model confirms the heterogeneity of the biosorbent surface, since $0 < n < 1$ at various temperatures.

A dimensionless separation factor K_L was calculated by Eq. (14) for confirmation of the efficiency of biosorption.

$$K_L = \frac{1}{1 + (k_{ads} \times C_o)} \quad (14)$$

where k_{ads} is the Langmuir constant (L/mg) and C_0 is the initial adsorbate concentration (mg/L).

Table 3
Equilibrium isotherm parameters for biosorption of Cr^{6+} onto SCB. (Metal concentration: 10–200 mg/L, SCB dosage: 10 g/L, pH: 2)

	Freundlich			Langmuir				Sips				Dubinin–Radushkevich			
T (°C)	n	k_F (L/g)	R^2	$q_{\max}$ (mg/g)	k_{ads} (L/mg)	k_L	R^2	$q_{\max}$ (mg/g)	K_{ads} (L/mg)	n	R^2	$q_{\max}$ (mg/g)	k_{D-R} (mol^2/kJ^2)	E (kJ/mol)	R^2
25	1.76	0.27	0.99	1.76	0.08	0.6	0.99	1.62	0.0081	0.50	0.99	2.53	$4.48 \cdot 10^{-3}$	10.6	0.80
50	2.71	0.21	0.82	1.30	0.07	0.8	0.99	1.16	0.016	0.61	0.98	1.44	$3.57 \cdot 10^{-3}$	11.8	0.87
65	2.52	0.18	0.84	1.28	0.05	0.7	0.99	1.21	0.036	0.84	0.94	1.66	$3.48 \cdot 10^{-3}$	12.0	0.88

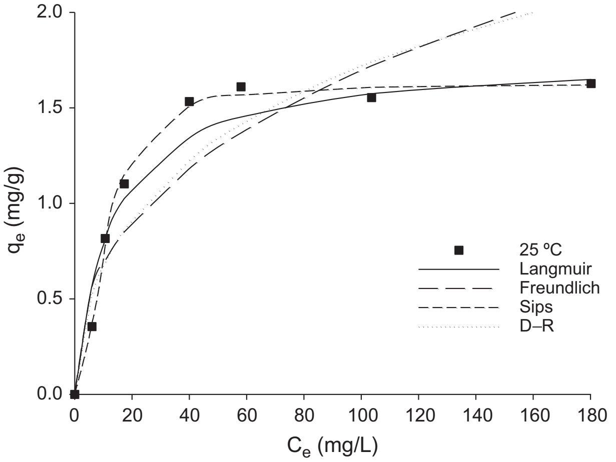

Fig. 9. Equilibrium isotherm for Cr^{6+} biosorption by SCB. (Metal conc.: 10–200 mg/L, SCB dosage: 10 g/L, temp: 25˚C, pH: 2).

Table 4
Thermodynamic parameters for the biosorption of Cr^{6+} on SCB (Measured between 25 and 65˚C)

Biosorbent: SCB		ΔG (kJ mol^{-1})	ΔH (kJ mol^{-1})	ΔS (kJ $mol^{-1}.K^{-1}$)
Temperature (˚C)	25	−20.44	−6.364	−0.0102
	50	−21.87		
	65	−22.87		

$0 < K_L < 1$ denotes favorable biosorption and $K_L > 1$ is an indication of unfavorable biosorption [19].

The values for K_L listed in Table 3 were calculated for 10 mg/L initial concentration, which is the lowest initial Cr^{6+} concentration applied for isotherm studies. The values of K_L are all in the range 0–1, which indicates the favorability of Cr^{6+}biosorption by SCB.

The Fig. 9 presents the adjustment of the experimental data to the four models used for the biosorption of Cr^{6+} onto SCB at 25˚C.

The Langmuir model is the one which better reproduces the experimental results and these results are analogous to those obtained by the model of Sips. The values of the parameter n of the isotherm of Sips approach unity, which ratifies that in these conditions, the model of Sips tends to resemble the isotherm of Langmuir in the range of concentrations studied.

The $q_{\max}$ values obtained (1.76 mg/g) showed that initial pH of the solution (pH 2) affected the uptake capacity of the SCB, due to which a very high Cl^- ion concentration (0.01 mol/L) in the solution may compete with $HCrO_4^-$ ($2.5.10^{-4}$ mol/L) and the binding of the primary metal ions decreases [47].

Similar results have also been reported for the biosorption of Cr^{6+} on sawdust (0.229 mg/g) [48], pine leaves (0.277 mg/g) [45], raw rice (0.07 mg/g) [49], and modified oak sawdust (1.7 mg/g) [50]. Although, a direct comparison of biomass with other reported biosorbents is difficult, due to the varying experimental conditions employed in those studies.

3.5. Thermodynamic evaluation of the process

Thermodynamic parameters, such as free energy of biosorption (ΔG), enthalpy (ΔH), and entropy (ΔS) can be evaluated from the following equations on a temperature range of 25–65˚C [19,21,51,52]:

$$\Delta G = -RT \ln k_{\text{ads}} \tag{15}$$

$$\ln k_{\text{ads}} = \frac{\Delta S}{R} - \frac{\Delta H}{RT} \tag{16}$$

$$\Delta S = \frac{\Delta H - \Delta G}{T} \tag{17}$$

where k_{ads} is the Langmuir constant (L/mol).

The values of these parameters are summarized in Table 4. For the SCB biosorbent studied, the enthalpy change (ΔH) is negative (exothermic) due to decrease in biosorption with successive increases in temperature. Further, negative (ΔG) values indicate the spontaneous nature of the biosorption process and negative values of (ΔS) reveal the decreased randomness at the solid–solution interface during the fixation of the Cr^{6+} on the active sites of the biosorbent.

4. Conclusions

- The Cr^{6+} biosorption onto SCB was favored by pH 2, temperature 25˚C, and with 10 g/L biosorbent dosage.
- The kinetic studies indicated that equilibrium in the biosorption of Cr^{6+} onto SCB was reached in 90 min of contact time and revealed that the kinetic biosorption data are well-fitted to the pseudo-second-order kinetic model.
- The biosorption isotherms followed the Langmuir model. The maximum biosorption capacity of Cr^{6+} for SCB was 1.76 mg/g at pH 2 and 25˚C.
- Biosorption energies calculated with the D–R model were found to be between 8 and 16 kJ/mol suggesting the chemisorption nature of the biosorption process.

- Thermodynamic studies indicated that the process of biosorption of Cr^{6+} by SCB was feasible, spontaneous, and exothermic in nature.

Acknowledgment

The authors are grateful to the alpha BIOPROAM Program Contract No. AML/190901/06/18414/II-0548-FC-FA.

References

[1] N. Tewari, P. Vasudevan, B.K. Guha, Study on biosorption of Cr(VI) by *Mucor hiemalis*, Biochem. Eng. J. 23 (2005) 185–192.

[2] E. Oguz, Adsorption characteristics and the kinetics of the Cr (VI) on the *Thuja Oriantalis*, Colloids Surf. A 252 (2005) 121–128.

[3] H. Zghida, M. Hassen, V. Baouab, R. Gautheir, Sorption of chromium oxy-anions onto cationized lingo-cellulosic material, J. Appl. Polym. Sci. 87 (2003) 1660–1665.

[4] S. Arivoli, B.R. Venkatraman, T. Rajachandsekar, M. Hema, Adsorption of ferrous ion from aqueous solution by low cost activated carbon obtained from natural plant material, Res. J. Chem. Environ. 17 (2007) 70–78.

[5] G. Blázquez, M.A. Martin-Lara, E. Dionisio-Ruiz, G. Tenorio, M. Calero, Evaluation and comparison of the biosorption process of copper ions onto olive stone and pine bark, J. Ind. Eng. Chem. 17 (2011) 824–833.

[6] M. Gavrilescu, Removal of heavy metals from the environment by biosorption, Eng. Life Sci. 4 (2004) 219–232.

[7] F. Umar, A. Janusz, M.A.K. Kozinski, A. Makshoof, Biosorption of heavy metal ions using wheat based biosorbents, Bioresour. Technol. 101 (2010) 5043–5053.

[8] G. Blázquez, M. Calero, F. Hernáinz, G. Tenorio, M.A. Martín-Lara, Batch and continuous packed column studies of chromium(III) biosorption by olive stone, Environ. Prog. Sustain. 30 (2011) 576–585.

[9] M.A. Martín-Lara, G. Blázquez, A. Ronda, I.L. Rodríguez, M. Calero, Multiple biosorption–desorption cycles in a fixed-bed column for Pb(II) removal by acid-treated olive stone, J. Ind. Eng. Chem. 18 (2012) 1006–1012.

[10] A.E. Okoronkwo, S.J. Olusegun, Biosorption of nickel using unmodified and modified lignin extracted from agricultural waste, Desalin. Water Treat. 51 (2012) 1989–1997.

[11] Y. Ding, D. Jing, H. Gong, L. Zhou, X. Yang, Biosorption of aquatic cadmium(II) by unmodified rice straw, Bioresour. Technol. 114 (2012) 20–25.

[12] P.S. Saha, A. Dey, P. Marik, Batch removal of chromium (VI) from aqueous solutions using wheat shell as adsorbent: Process optimization using response surface methodology, Desalin. Water Treat. 39 (2012) 95–102.

[13] Y. Chen, L. Ding, J. Nie, Isotherm and thermodynamic studies of the biosorption of lead, cadmium and copper from aqueous solutions by rice bran, Desalin. Water Treat. 44 (2012) 168–173.

[14] D. Harikishore Kumar Reddy, K. Seshaiah, A.V.R. Reddy, S. M. Lee, Optimization of Cd(II), Cu(II) and Ni(II) biosorption by chemically modified Moringa oleifera leaves powder, Carbohydr. Polym. 88 (2012) 1077–1086.

[15] K.M. Doke, M. Yusufi, R.D. Joseph, E.M. Khan, Biosorption of hexavalent chromium onto wood apple shell: Equilibrium, kinetic and thermodynamic studies, Desalin. Water Treat. 50 (2012) 170–179.

[16] S.C. Ibrahim, M.A.K.M. Hanafiah, M.Z.A. Yahya, Removal of cadmium from aqueous solutions by adsorption onto sugarcane bagasse, American-Eurasian J. Agric. Environ. Sci. 1 (2006) 179–184.

[17] O. Karnitz, L.V.A. Gurgel, J.C.P. De Melo, V.R. Botaro, T.M.S. Melo, R.P. de Freitas Gil, L.F. Gil, Adsorption of heavy metal ion from aqueous single metal solution by chemically modified sugarcane bagasse, Bioresour. Technol. 98 (2007) 1291–1297.

[18] I. Alomá, M.A. Martín-Lara, I.L. Rodríguez, F. Blázquez, M. Calero, Removal of nickel (II) ions from aqueous solutions by biosorption on sugarcane bagasse, J. Taiwan Inst. Chem. Eng. 43 (2012) 275–281.

[19] Inés de la C. Alomá, Tecnología sostenible para la obtención de un biosorbente de metales pesados a partir del bagazo de caña de azúcar [Sustainable technology for the production of a heavy metal biosorbent from sugarcane bagasse]. Tesis en opción del grado de Doctor en Ciencias Técnicas, Departamento Ingeniería Química, Universidad Central "Marta Abreu "de las Villas, Cuba, 2011.

[20] R. Sips, Structure of a Catalyst Surface, Chemical Instrumental Nueva Editorial Interamericana, México, 1948.

[21] J.E. Basurco Cayllahua, R.J. de Carvalho, M.L. Torem, Evaluation of equilibrium, kinetic and thermodynamic parameters for biosorption of nickel(II) ions onto bacteria strain, *Rhodococcus opacus*, Miner. Eng. 22 (2009) 1318–1325.

[22] M.A. Martín-Lara, I.L. Rodriguez, Inés de la C. Alomá, G. Blázquez, M. Calero, Modification of the sorptive characteristics of sugarcane bagasse for removing lead from aqueous solutions, Desalination 256 (2010) 58–63.

[23] F. Cortés, Evaluación del impacto ambiental que provoca la tecnología empleada para la obtención y uso de un biosorbente de metales pesados a partir del bagazo de caña químicamente activado [Evaluation of environmental impact caused by the used technology to the obtention and the use of a biosorbent of heavy metals from chemically treated sugarcane bagasse]. Tesis en opción al grado de Master en Ingeniería en Saneamiento Ambiental, Departamento Ingeniería Química, Universidad Central "Marta Abreu" de Las Villas, Cuba, 2006.

[24] J. Brito, Propuesta de una tecnología para obtener un biosorbente de Cr^{3+} a partir del bagazo de caña. Escalado a nivel de planta piloto [A technology to obtain a biosorbent for Cr^{3+} from sugarcane bagasse. Plant pilot scale-up]. Tesis en opción al grado Master en Análisis de Proceso, Departamento de Ingeniería Química, Universidad Central "Marta Abreu" de Las Villas, Cuba, 2006.

[25] H. Teng, Y. Wei, Thermogravimetric studies on the kinetics of rice husk pyrolysis and the influence of water treatment, Indian Eng. Chem. Res. 37 (1998) 3806–3811.

[26] Y.C. Sharma, C.H. Weng, Removal of chromium(VI) from water and wastewater by using riverbed sand: Kinetic and equilibrium studies, J. Hazard. Mater. 142 (2007) 449–454.

[27] Inés de la C. Alomá, Evaluación de la operación de adsorción de metales pesados empleando columnas rellenas con bagazo de caña químicamente modificado y propuesta de escalado a nivel de planta piloto [Evaluation of heavy metals adsorption using packed-bed-columns with chemically modified sugarcane bagasse and the proposal of scale-up pilot plant]. Tesis en opción al grado Master en Ingeniería en Saneamiento Ambiental, Departamento de Ingeniería Química, Universidad Central "Marta Abreu" de Las Villas, Cuba, 2006.

[28] Y. González, I.L. Rodríguez, E. Guibal, M. Calero, M.A. Martín-Lara, Biosorption of hexavalent chromium from aqueous solution by *Sargassum muticum* brown alga. Application of statistical design for process optimization, Chem. Eng. J. 183 (2012) 68–76.

[29] O.D. Uluozlu, A. Sarı, M. Tuzen, M. Soylak, Biosorption of Pb(II) and Cr(III) from aqueous solution by lichen (*Parmelina tiliaceae*) biomass, Bioresour. Technol. 99 (2008) 2972–2980.

[30] M. Erdem, H.S. Altundogan, F. Tumen, Removal of hexavalent chromium by using heat-activated bauxite, Miner. Eng. 17 (2004) 1045–1052.

[31] Z. Sadaoui, S. Hemidouche, O. Allalou, Removal of hexavalent chromium from aqueous solutions by micellar compounds, Desalination 249 (2009) 768–773.

[32] S. Lagergren, About the theory of so-called adsorption of soluble substances, K. Sven. Vetenskapsakad. Handl. 24 (1898) 1–39.

[33] Y.S. Ho, G. McKay, Sorption of dye from aqueous solution by peat, Chem. Eng. J. 70 (1978) 115–124.

[34] W.J. Weber, J.C. Morris, Advances in Water Pollution Research: Removal of Biologically Resistant Pollutant from Waste Water by Adsorption, International Conference on Water Pollution Symposium, vol. 2, Pergamon, Oxford 1962 pp. 231–266.

[35] Y.S. Ho, D.A.J. Wase, C.F. Forster, Kinetics studies of competitive heavy metal adsorption by sphagnum moss peat, Environ. Technol. 17 (1996) 71–77.

[36] M. Stanley, Environmental Chemistry, 4th ed., Lewis, Boston, MA, pp. 155 1990.

[37] Y.S. Ho, S.G. McKay, Pseudo-second order model for sorption processes, Process Biochem. 34 (1999) 451–465.

[38] I. Langmuir, The adsorption of gases on plane surfaces of glass, mica and platinum, J. Am. Chem. Soc. 40 (1918) 1361–1403.

[39] Y.A. Aydın, N.D. Aksoy, Adsorption of chromium on chitosan: Optimization, kinetics and thermodynamics, Chem. Eng. J. 151 (2009) 188–194.

[40] T.S. Singh, K.K. Pant, Equilibrium, kinetics and thermodynamic studies for adsorption of As (III) on activated alumina, Sep. Purif. Technol. 36 (2004) 139–147.

[41] S.P. Dubey, K. Gopal, Adsorption of chromium(VI) on low cost adsorbents derived from agricultural waste material: A comparative study, J. Hazard. Mater. 145 (2007) 465–470.

[42] H. Freundlich, Colloid and Capillary Chemistry, Methuen, London, UK, 1926.

[43] M.M. Dubinin, The potential theory of adsorption of gases and vapors for adsorbents with energetically non-uniform surface, Chem. Rev. 60 (1960) 235–236.

[44] V. Sarin, K.K. Pant, Removal of chromium from industrial waste by using eucalyptus bark, Bioresour. Technol. 97 (2006) 15–20.

[45] A. Sari, M. Tuzen, Biosorption of total chromium from aqueous solution by red algae (*Ceramium virgatum*): Equilibrium, kinetic and thermodynamic studies, J. Hazard. Mater. 160 (2008) 349–355.

[46] A. Sari, M. Tuzen, Removal of Cr(VI) from aqueous solution by Turkish Vermiculite: Equilibrium, thermodynamic and kinetic studies, Sep. Sci. Technol. 43 (2008) 3563–3581.

[47] B. Volesky, Sorption and Biosorption, BV Sorbex, Montreal, 2003.

[48] K. Morshedzadeh, H.R. Soheilizadeh, S. Zangoie and M. Aliabadi, Removal of chromium from aqueous solutions by lignocellulosic solid wastes, 1st. Environment conference, Tehran University, Department of Environment Engineering, 2007.

[49] E.A. Oliveira, S.F. Montanher, A.D. Andrade, J.A. Nobrega, M.C. Rollemberg, Equilibrium studies for the sorption of chromium and nickel from aqueous solutions using raw rice bran, Process Biochem. 40 (2005) 3485–3490.

[50] M.E. Argun, S. Dursun, C. Ozdemir, M. Karatas, Heavy metal adsorption by modified oak sawdust: Thermodynamics and kinetics, J. Hazard. Mater. 141 (2006) 77–85.

[51] Y.S. Ho, Removal of copper ions from aqueous solution by tree fern, Water Res. 37 (2003) 2323–2330.

[52] K.K. Singh, A.K. Singh, S.H. Hasan, Low cost biosorbent wheat bran for the removal of cadmium from wastewater: Kinetic and equilibrium studies, Bioresour. Technol. 97 (2006) 994–1001.